Pharmaceutical Research, Vol. 27, No. 2, February 2010 (© 2009)
DOI: 10.1007/s11095-009-0023-z

Research Paper

Therapeutic Potential of New 4-hydroxy-tamoxifen-Loaded pH-gradient Liposomes in a Multiple Myeloma Experimental Model

Giorgia Urbinati,[1,2,3] Davide Audisio,[2,3,4] Véronique Marsaud,[1,2,3] Vincent Plassat,[1,2,3] Silvia Arpicco,[5] Brigitte Sola,[6] Elias Fattal,[1,2,3,7] and Jack-Michel Renoir[1,2,3,8]

Received July 30, 2009; accepted December 1, 2009; published online December 23, 2009

Purpose. To determine the better liposomal formulation incorporating the active metabolite of tamoxifen, 4-hydroxy-tamoxifen (4HT) and the biological impact of 4HT-pH-gradient liposomes on response to *in vivo* treatment.
Methods. Several pegylated liposomes were formulated by varying the composition of lipids, increasing external pH from 7.4 to 9.0 and doubling the lipid concentration. Dipalmitoylphosphatidylcholine / cholesterol / distearoylphosphoethanolamine poly(ethylene)glycol liposomes (DL-9 liposomes) were chosen for their physico-chemical properties. Toxicity and release kinetics were assessed in breast cancer MCF-7 as well as in multiple myeloma (MM) cells. *In vivo* antitumor activity and bio-distribution were measured in the RPMI8226 MM model.
Results. Compared to conventional non-pH-gradient liposomes, 4HT-DL-9 liposomes resulted in concentration of up to 1 mM 4HT, greater stability, relative toxicity and slow 4HT release. Intravenous injections of 4HT-DL-9 liposomes at 4 mg/kg/week blocked MM tumor growth. Ki67 and CD34 labeling decreased in treated tumors, concomitantly with increase of activated caspase-3 supporting a cell proliferation arrest, a decrease of tumor vasculature and the induction of tumor cell death.
Conclusion. This antitumor effect was assumed to be the result of a modified biodistribution of 4HT once trapped in DL-9 liposomes. Such 4HT-containing pH-gradient Stealth® nanocarriers could be helpful for MM treatment.

KEY WORDS: breast cancer; hydroxy-tamoxifen; multiple myeloma; pH-gradient Stealth® liposomes.

INTRODUCTION

Tamoxifen (Tam), a member of the Selective Estrogen Receptor Modulator (SERM) family, is the treatment of choice at all stages of estrogen receptor (ER)-positive (ER+) breast cancer and can prevent breast cancer in women at risk (1,2). Like all SERMs with a triphenyl ethylene skeleton, Tam and its active metabolite 4-hydroxy-tamoxifen (4HT) counteract the proliferative effects of estradiol (E_2) in the mammary gland and induce breast cancer cell death (3–5). SERMs may exhibit an agonistic or antagonistic activity on ER depending on the cellular context. For example, Tam and Raloxifen both behave as ER antagonists in breast and agonists in bones, but only Tam manifests agonistic activity in the uterus (6), where its effects are linked to incidence of endometrial cancers (7). ER is a transcription factor which belongs to the steroid/thyroid nuclear hormone receptor family and is activated through binding to agonist ligands (8). Despite the fact that the majority of ER+ breast cancers maintain their hormonal dependency (9,10), ER-negative tumors may respond to Tam (11,12). This suggests that Tam is active independently of ER. Recently, it has been proposed that induction of cell death and/or autophagy by antiestrogens in breast cancer cells may occur, at least in part, through modulation of cholesterol metabolism following binding of SERMs that contain an aminoethoxy side chain like Tam, to the microsomal antiestrogen binding site (AEBS) (13).

Multiple myeloma (MM) is an incurable B hemopathy with a median survival of 2–3 years, characterized by malignant plasma cells accumulating in the bone marrow and by the development of osteolytic lesions (14). A large number of MM tumor cells have also been shown to express ER, although expression levels are much lower and more varied compared to breast cancer. Depending on the cell line,

[1] CNRS, UMR 8612, Physico-Chimie, Pharmacotechnie, Biopharmacie, Laboratoire Pharmacologie Cellulaire et Moléculaire des Anticancéreux, Faculté de Pharmacie, 5 rue J.B. Clément, Châtenay-Malabry, F-92296, France.
[2] University Paris-Sud, Orsay, F-91405, France.
[3] IFR 141, Châtenay-Malabry, F-92296, France.
[4] CNRS, BIOCIS-UMR 8076, Laboratoire de Chimie Thérapeutique, Châtenay-Malabry, F-92296, France.
[5] Facoltà di Farmacia, Università degli studi di Torino, via Pietro Giuria, Torino, Italy.
[6] Biologie Moléculaire et Cellulaire de la Signalisation, EA 3919, IFR186, Université de Caen Basse Normandie, 14000, Caen, France.
[7] CNRS, UMR 8612, Laboratoire de Vectorisation Pharmaceutique de Molécules fragiles, 5 rue J.B. Clément, Châtenay-Malabry, F-92296, France.
[8] To whom correspondence should be addressed. (e-mail: michel.renoir@u-psud.fr)

ABBREVIATIONS: Chol, Cholesterol; DPPC, Dipalmitoylphosphatidylcholine; DSPC, 1,2-distearoyl-sn-glycero-3-phosphatidylcholine; DSPE-PEG_{2000}, 1,2-distearoyl-sn-glycero-3-phosphoethanolamine-N-[methoxy(Polyethyleneglycol)-2000] (ammonium salt); ePC, egg-phosphatidylcholine; ePG, egg-phosphatidylglycerol; ER, estrogen receptor; 4HT, 4-hydroxy-tamoxifen.

different AEs arrest progression of the cell cycle and/or induce apoptosis (15–17). For examples, 4HT arrests cell cycle and induces apoptosis in LP-1 MM cells, while the selective estrogen receptor down-regulators (SERDs) RU 58668 (RU) and Faslodex® induce only apoptosis in RPMI8266 MM cells (17–19). Raloxifen acts like 4HT for arresting cell proliferation and inducing apoptosis in MM cells (20). AE-induced cell cycle arrest always occurs at nanomolar concentrations in breast cancer cells and is ER-dependent (21). By contrast, AE-induced cell death in both breast cancer and MM cells occurs at higher AE concentrations (between 5 to 10 μM). When administered at such elevated concentrations, AEs can differently affect various tissues in which ER is expressed; for instance, due to its agonistic activity, Tam can block osteoporosis in bone cells of menopausal women but triggers endometrium cancers in 1–2% of treated patients (7,22). Therefore, in order to avoid detrimental effects of Tam, there is a need for a system capable of delivering it at high concentration in the desired cell tissue. In addition, for a therapeutic approach, it warrants use of the active metabolite of Tam, 4HT, rather than the prodrug, which is 50–100-fold less active in cancer cells and which suppresses cell proliferation less effectively than 4HT does (23,24). For this purpose, AE-loaded nanocarriers have been thought to constitute promising therapeutic tools.

Various drug delivery nanocarriers incorporating Tam have been widely developed in the past. Among them, Stealth® nanocarriers for intravenous administration have appeared promising therapeutics in animal models. They were based on nanoparticles which incorporated either Tam itself (25–30) or 4HT (31) as well as RU (32,33). However, polymer-based nanoparticle systems display low Tam loading, and the drug tends to be surface-bound, resulting in rapid release characteristics. Lipid vesicles were also used for the entrapment of Tam or 4-HT (34–36), and lack of incorporation of Tam was observed by using cyclodextrin and polysaccharide-based nanogels contrary to another hydrophobic molecule such as benzophenone (37). We then designed an appropriate drug delivery system to improve 4HT loading efficiency and reduce the drug back-diffusion from liposomes. We chose to develop a pH-gradient liposomal system, a type of liposome first described more than ten years ago for the incorporation of amino-containing anticancer drugs such as doxorubicin (38–40), gemcitabine (41,42), topotecan (43), vincristine (44,45) and irinotecan (46). The concept takes advantage of the different behavior that molecules (weak acids and bases) have once they are protonated (41). Because of its amine group, 4HT is charged at acidic pH and neutral once the pH is basic. If the external pH of the system results to be basic, the molecule will tend to be uncharged, and because of its lipophylic properties, it will be able to cross the lipid barrier of liposomes. Once inside the core of liposomes, it will get protonated, thus unable to escape from the aqueous core of the vesicle. Such a transmembrane pH-gradient method is then supposed to promote the 4HT encapsulation and retain the molecule longer than other conventional liposomes. We have formulated several 4HT-containing pH-gradient liposomal systems, varying lipid concentrations and pH values. We then compared their characteristics with those of conventional liposomes. In the present study, we optimized a new liposomal formulation incorporating a high concentration of 4HT and determined the resulting cytotoxic effects on MM cells as compared to the classical MCF-7 breast cancer cell line. The antitumor activity of the new pH-gradient 4HT-loaded liposomal nanosystem obtained was biologically evaluated *in vivo* on a MM animal model. Preliminary data indicate a strong reduction of the tumor growth, correlated with enhanced tumor accumulation of 4HT, suggesting a promising therapeutical effect.

MATERIALS AND METHODS

Materials

Lipids DPPC[1], DSPC, Chol and MTT tetrazolium salt were obtained from Sigma Aldrich (St. Quentin-Fallavier, France). ePC and ePG were obtained from Lipoid GmbH (Ludwigshafen, Germany). DSPE-PEG_{2000} was purchased from Avanti Polar Lipids (Alabaster, AL, USA). One gram of 4HT was obtained from Besins Iscovesco. Sephacryl S-1000 Superfine was purchased from GE Healthcare (Sweden). HPLC Discovery® C8 column (15 cm×4.6 mm, 5 μm particles) and Discovery Supelguard Catridge for the C8 column were purchased from Supelco-Sigma-Aldrich group (St-Quentin, France). Spectra/Por dialysis tubing was obtained from Spectrum Laboratories, Rancho Dominguez, CA, USA). All other laboratory chemicals were reagent grade, purchased from standard suppliers.

Preparation of Liposomes

Conventional Stealth Liposomes

Liposome suspensions (50 mM lipids) were prepared by a procedure previously described (33). Lipid film hydration was performed at the following molar ratios: ePC/Chol/DSPE-PEG_{2000} (64:30:6), DPPC/Chol/DSPE-PEG_{2000} (64:30:6), DPPC/DSPE-PEG_{2000} (94:6) and DPPC/ePG/DSPE-PEG_{2000} (84:10:6). Incorporation of 4HT in liposomes was obtained by mixing the AE (1.25 mM initial concentration) with chloroformic lipid solution. The lipid film was resuspended in Hepes buffer (Hepes 10 mM, NaCl 145 mM, pH 7.4). Multivesicular suspensions were then extruded (extruder Whitley, Lipex, Vancouver, Canada) sequentially through 0.2 and 0.1 μm polycarbonate membranes (Millipore, USA). Unincorporated 4HT was then eliminated by gel filtration as described below for the pH-gradient liposomes. The concentration of 4HT incorporated in purified liposomes was determined by UV spectroscopy at 287 nm after lipid solubilization in ethanol.

pH-gradient Liposomes

4HT contains an alkylic amine, which is 90% ionized at pH 7.4, the usual pH of hydration buffer. Different pH-gradient liposome formulations were prepared in order to obtain an optimized formulation (small size, high drug encapsulation efficiency, low toxicity, high stability). Lipids were mixed at the chosen ratios to constitute the lipidic film. Lipid mixtures were then subjected to hydration and dialysis at the desired pH. Liposomes containing 19 mM (L lip-

osomes) or 38 mM lipids (DL liposomes) were prepared by lipid film hydration at the molar ratio: DSPC/Chol/DSPE-PEG_{2000} (64:30:6). The dried lipidic film was suspended in an ammonium sulphate solution $(NH_4)_2SO_4$ (250 mM, pH 5.1) and vortexed for 30 min at 60°C. Following hydration, the multilamellar vesicles (MLVs) were subjected to five freeze-thaw cycles (freezing in liquid nitrogen and thawing at 60°C) in order to improve liposome permeability and homogenize the distribution of ammonium charges (41). Samples were extruded 10 times through stacked polycarbonate filters with 0.2 and 0.1 µm pores at 60°C; the resulting suspension was introduced into a 10-cm piece of Spectra/Por dialysis tubing (MW cut-off 10.000). Non-entrapped $(NH_4)_2SO_4$ was removed by dialyzing the sample against a 500-fold excess of Hepes buffer (Hepes 25 mM, NaCl 150 mM, pH 7.4 or 9) at 4°C overnight under gentle stirring. These conditions allow the formation of a pH gradient with an acidic environment in the intra-liposomal aqueous compartment (38–40).

An ethanol solution of 4HT (10 mg/ml) in Hepes buffer (pH 7.4 or 9.0) was then added to the liposomal formulation (1.25 mM final concentration, v/v 1:1), ensuring that the ethanol volume did not exceed 10% of the final liposome volume. The liposome formulation supplemented with 4HT was then heated for 5, 15, 30 min and 1 h at 60°C to determine the higher encapsulation rate. The 4HT concentration was determined by HPLC and the encapsulation rate calculated as follows: final drug concentration incorporated / initial drug concentration added x 100.

Cell Culture and Treatments

MM RPMI 8226 cells grew in RPMI 1640 medium (Eurobio, Les Ullis, France) supplemented with 10% fetal calf serum (FCS). At least 2 days before treatments, both media were replaced by phenol red-free medium supplemented with 10% stripped FCS (charcoal Norit A 1%, Dextran T70 0.1%, 30 min at room temperature), L-glutamine (2 mM), penicillin (50 UI/mL) and streptomycin (50 UI/mL). Human breast cancer MCF-7 cells were obtained from American Type Culture Collection (Manassass, VA, USA); MELN cells are MCF-7 cells stably expressing the ERE-β globin-luciferase construct (47,48). Breast cancer (BC) cells were grown in Dulbecco's Modified Eagle Medium (DMEM, Lonza, Vervier, Belgium) supplemented with 10% FCS, L-glutamine (2 mM), and penicillin/streptomycin (50 U/mL/50 µg/mL).

Cell viability was determined by MTT assay. Briefly, cells (10^4 per well) were seeded onto 96-well plates and incubated with pH-gradient loaded liposomes or free 4HT for various times. MTT was added (100 µg/well) for 2 h incubation at 37°C. The medium was then removed, and formazan crystals were dissolved in 200 µL DMSO. The absorbance of converted dye, which correlates with the number of viable cells, was measured at 570 nm, with subtraction of background absorbance at 650 nm, using a microplate reader (Metertech Σ 960, Fisher Bioblock, Illkirch, France).

Drug Encapsulation Efficiency

The non-entrapped 4HT was removed by gel permeation chromatography on a Sephacryl S1000 column (100 µl sample volumes were placed on columns with at least a 1 ml column bed). Hepes buffer at pH 7.4 or 9.0, depending on the preparation, was used as the mobile phase. The amount of 4HT entrapped in liposomes was measured by HPLC. Briefly, liposomes (100 µL) were disrupted using 500 µL of acetonitrile. The resulting solution was filtered through a 0.22 µm syringe filter to remove the precipitate and transferred into HPLC vials. Various known concentrations of free 4HT were also filtered to verify that there was no loss during the filtration step. The mobile phase used for the C8 reverse phase column was a methanol / KH_2PO_4 buffer (10 mM, pH 5) (7:3 v/v). Chromatographic analysis was carried out at room temperature at a 1 ml/min flow rate. A calibration curve was determined for known 4HT concentrations, and optical densities were read at λmax of 287 nm. The percentage of encapsulated 4HT was calculated from the amount of encapsulated 4HT divided by the amount of 4 HT added at the beginning of the fabrication process multiplied by 100.

Physico-chemical Characterization of the Liposomes

The hydrodynamic diameter and the zeta potential of the particles (means ± SD) from three independent preparations were measured in triplicate (Zetasizer 4, Malvern Instruments, Ltd, France) as described previously (49).

4HT Release Kinetics

Since the level of ER-mediated transcription in MELN cells is E_2-dependent and dose-dependently inhibited by 4HT, we used MELN cells (48) for evaluating the release of 4HT from liposomes. Cells at 50–60% confluence were seeded in 3-cm diameter Petri dishes maintained at 37°C under 5% CO_2 in a 95% humidified atmosphere. Free or incorporated 4HT were placed for various periods of time in inserts (NUNC Anapore, membrane 0.02 µm, Nalge Nunc Inc., USA) in the presence of 0.1 nM E2. Only free 4HT and E_2 could pass through the insert membrane. Following incubation of cells with free or entrapped 4HT, inserts were then removed from the dishes, and cell culture was maintained at 37°C for a final incubation time of 24 h. Cells were then rinsed in PBS and lysed in 250 µL of buffer containing 25 mM Tris/HPO_4, 10 mM $MgCl_2$, 1% Triton X100, 15% glycerol and 1 mM EDTA (pH 7.8) on ice for 30 min. Cell lysates were cleared by centrifugation (10 min, 14,000 rpm at 4°C). Luciferase activity was quantified in a luminometer (Lumat LB 9507, Berthold, France), after injection of the luciferase buffer (100 µl) supplemented with 100 mM ATP and 87 µg luciferin/ml, to 100 µl of cellular extract. For controls, MELN cells were treated with E_2 (0.1 nM) to obtain 100% transcription and with empty liposomes or a 100-fold molar excess of free 4HT in order to inhibit completely E2-induced luciferase expression (50).

Flow Cytometry

Cells (1–1.5×10^5 cells/ mL) were cultured in the presence or not of free 4HT, or 4HT-loaded pH-gradient liposomes (1 and 10 µM each), or with unloaded liposomes at the same lipid concentration. After treatment, cells were washed and fixed in PBS/ethanol (30/70). For flow cytometric examination, cells (10^4) were incubated for 30 min in PBST containing 0.2% triton X100, 1 mM EDTA and propidium iodide (PI, 50 µg/

mL) supplemented by RNase (0.5 mg/mL). Analyses were performed with a FACS Calibur (Becton Dickinson, Le Pont de Claix, France). Cell Quest software was used for data acquisition and analysis.

Xenografts

We used the RPMI 8226 model described previously (33). Briefly, female nude mice (5–6 week-old, Janvier France) were s.c. inoculated with 10^7 cells half mixed in Matrigel (BD Bioscience, Le Pont de Claix, France). Tumors developed over a period of 5 to 7 weeks, reaching sizes of 300 to 500 mm^3 (calculated as 1/2 (width × length^2)). Mice (6 per group) were then i.v. injected twice a week with free 4HT (4 mg/kg/week) dissolved in 0.9% NaCl containing 5% glucose, 4HT-loaded pH-gradient liposomes (4 mg 4HT/kg/week) or unloaded liposomes (at the same lipid concentration as that of the 4HT-loaded liposomes). Six more mice were not injected and served as control for growth of untreated tumors. During experiments, mice were maintained in accordance with the principles of the Declaration of Helsinki and in respect of the French legislation on animal welfare. At the end of the experiment, tumors were excised and immediately fixed in Finefix (Milestone s.r.l., Sorisole, Italy) prior to dehydratation and paraffin inclusion for immunohistochemistry.

Biodistribution

For this experiment, conventional 4HT-liposomes and pH-gradient DL-9 liposomes containing 1 mM 4HT isotopically diluted at 1/215 000 dilution in ^{3}H-4HT (85 Ci/ mmole) were i.v. injected (10^6cpm / 200 µL) in xenografts (n=3 per group). The capacity of these liposomes to distribute in the organism was measured 1 and 24 h after injection and compared with the biodistribution of free ^{3}H-4HT (same amount) diluted in 5% glucose in PBS (G5). The liver, spleen, lung, uterus and tumor were removed, weighted and placed in 1 mL of Soluene-350 solution (Packard Bioscience, Rungis, France) overnight at 50–60°C. Then 0.1 mL H_2O_2 (30%) was added for bleaching. After digestion, samples (500 µL) were supplemented with scintillation solution (HIONIC-FLUOR, Perkin-Elmer, Boston, MA, USA) and counted in a Beta scintillation counter with standard measurement.

Immunohistochemistry

Paraffin sections were xylene-treated then rehydrated. Following antigen retrieval in citrate buffer pH6.2 (5 min at 85°C), immunohistochemistry of the proliferative marker Ki67 (mouse anti-human M7240 Dako, Denmark; 1/75 diluted), the cleaved caspase-3 (rabbit anti-human Ab clone 9661S, Cell Signaling, In Vitrogen; 1/200 diluted), and the murine endothelial cells (anti-mouse CD34$^+$Ab clone MEC14.7, HyCult biotechnology b.v., The Nederlands; 1/20 diluted) was performed using the Vector Vectastain Elite kit (Biovalley, Conches, France) and the DAB as chromagen. Slices were counterstained with Mayer's hematoxilin and mounted (Eukitt, CML, Nemours, France).

Statistical Analyses

The student t test was used to determine the significance of differences between two experimental groups. Mean of triplicates were analyzed by a two-sided test, and $P<0.05$ was considered significant. Repeated measures ANOVA test was used for comparison of tumor proliferation groups in animal experiments.

RESULTS AND DISCUSSION

Physicochemical Characteristics of Liposomes

Conventional Liposomes

Preliminary experiments using the liposome formulation ePC/Chol/DSPE-PEG, 64/30/6 in which the SERD RU was incorporated at a high concentration demonstrated a strong antitumor activity in a MM xenograft model (33). This formulation released slowly RU, but when RU was substituted by 4HT, despite a high loading (Table IA), a fast release of 4HT was observed (see below). We then further replaced ePC by DPPC, a lipid with a more rigid fatty acid chain. Given the positive charge of 4HT at pH 7.4, a negatively charged lipid (ePG) was also introduced in the system to allow formation of an ionic interaction between the drug and the lipid and thus reduce the rapid burst release of 4HT. Table IA summarizes the size and zeta potential of ePC/Chol/DSPE-PEG (64:30:6), DPPC/Chol/DSPE-PEG (64:30:6), DPPC/DSPE-PEG (94:6) and DPPC:ePG:DSPE-PEG (84:10:6) liposomes. Liposome size was in the range of 110–150 nm, whether empty or loaded with 4HT, a value compatible with extravasation from tumor vessels following their i.v. injection (51,52). Liposomes composed of ePC/Chol/DSPE-PEG had the smallest size and highest encapsulation rate (equivalent to 1.1 mM 4HT). We did not observe a difference between the ζ potential of this formulation with that of empty and 4HT-loaded liposomes, suggesting that the drug had been incorporated into the inner core of the system. The two formulations containing DPPC instead of ePC had lower encapsulation rate (see Table IA). Moreover, their ζ potential did not appear significantly different. This was not the case for the DPPC:ePG:DSPE-PEG in which substitution of ePC by ePG in the DPPC:ePG:DSPE-PEG liposomes caused a marked reduction (−42.2 mV) of the net ζ potential of these DPPC:ePG:DSPE-PEG liposomes. This is due to an excess of negative charges provided by the phosphate groups of ePG. All the formulations incorporated a high amount of 4HT, from 324 µg/mg lipids (equivalent to 0.8 mM 4HT) for the less charged formulation and up to 435 µg/mg lipids (corresponding to 1.1 mM 4HT) for the formulation with the greatest load, displaying in such conditions a satisfactory encapsulation yield.

pH-gradient Liposomes

In preliminary experiments, both the size and zeta potential of the liposomes were measured at various steps of their fabrication (Table II). Whatever the step, and 4HT loading or not, no change in the size of the liposomes was observed. After dialysis of empty DL-9 liposomes, the ζ potential decreased from −10.8±7.9 mV to −22.2±7.1 mV.

Table I. Physico-chemical Characteristics of Conventional and pH-gradient Liposomes

A					
Conventional liposomes	4HT	mean diameter (nm)	Zeta potential (mV)	4HT µg/30 mg lipids	Encapsulation yield (%)
ePC:Chol:DSPE-EPG_{2000}	−	106±30	−25.6±5.9	/	/
	+	131±19	−26.5±5.8	435/40±8	90±1.65
DPPC:Chol:DSPE-PEG_{2000}	−	145±25	−23.6±7.2	/	/
	+	148±39	−19.4±6.7	324/38±6	67±1.21
DPPC:DSPE-PEG_{2000}	−	137±43	−26.2±10	/	/
	+	139±45	−18.3±9.7	353/43±7	73±1.41
DPPC:ePG:DSPE-PEG_{2000}	−	150±41	−48.9±7.9	/	/
	+	153±45.5	−42.2±11.6	397/43±10	82±2.12
B					
pH-gradient liposomes	4HT	diameter (nm)	Zeta potential (mV)	4HT µg/30 mg lipids	Encapsulation yield (%)
L-7.4	−	138±32	−21.3±6	/	/
	+	139±33	−11.9±6.5	50/15±1.9	6±3
L-9	−	136±31	−26.7±5	/	/
	+	145±35	−16±5.3	97/15±0.3	20±3
DL-7.4	−	148±32	−25.6±8	/	/
	+	144±26	−9.5±6.2	79/30±1.9	14±2
DL-9	−	141±19	−24±5.	/	/
	+	146±32	−10.6±6.2	306/30±4	63±4

A/ The mean diameter, the zeta potential, 4HT content of liposomes and encapsulation yield (% of the 4HT encapsulated / 4HT initially added) were measured. Results are expressed as the means (nm ± poly dispersity index width) for the size, means (mV ± Z deviation) for the Z potential, means (µg/30 mg lipids ± SD) for the charge and means(% ± SD) for the encapsulation yield from three measurements for at least three different liposome preparations. The physicochemical properties of empty (minus 4HT) corresponding liposomes are also shown. B/ Similar measurements for pH-gradient purified liposomes before or after 4HT encapsulation during 1 h at 60°C. L, liposomes with 19 mM lipid concentration obtained at a pH of 7.4 (L-7.4) or at a pH of 9.0 (L-9); DL, liposomes with the double (38 mM) lipid concentration obtained at pH 7.4 (DL-7.4) or pH 9.0 (DL-9).

This was explained by the removal of external ammonium positive charges of the sulfate solution used to create the internal acidic pH in the core of the lipidic vesicles. For gel filtration purified 4HT-DL-9 liposomes obtained after 5 min heating, the ζ potential was −23.9±7.6 mV, while for those obtained after 1 h heating, it increased up to −10.6±6.3 mV. A similar increment of ζ potential was observed between loaded and unloaded L and DL-liposomes after 1 h heating, whatever the pH (Tale IB). The ζ potential increase observed after 1 h heating is likely the result of an enhancement of the interactions between 4HT and the lipid bilayer. This increase reflects the presence of the positive charges of the protonated amine of 4HT at the surface of the liposomes. Heating the DL-9 liposomes at 60°C for more than 1 h (75, 90 and 120 min) led to less 4HT incorporation than 1 h and to appearance of a new peak eluting later from the HPLC column (not shown), indicating 4HT molecule alteration. According to these preliminary data, and to the level of 4HT encapsulation rate (see below Fig. 1), 1 h heating was chosen as the optimum time for 4HT-DL-9 liposomes fabrication. No difference in the mean diameter between L and DL liposomes (~140 nm) was noticed, whether in the presence or absence of encapsulated 4HT (Table IB). These physicochemical parameters did not change over 5 weeks of storage at 4°C (not shown), indicating a good stability.

Drug Loading Efficiency

Conventional Liposomes

A high drug loading efficiency was obtained for the conventional liposomes, in excess of 70%, and reaching 90% for the ePC:Chol:DSPE-PEG formulations (Table IA). Replacing ePC by DPPC conducted to a decrease of 4HT incorporation. This is explained by the stronger rigidity of lipid chains of DPPC, allowing less space for both 4HT and Chol. By

Table II. Variations of Physico-chemical Parameters of pH-gradient Liposomes During the Fabrication Steps

DL-9 liposomes	Diameter (nm)	zeta potential (mV)
Empty DL-9 before dialysis	142±31	−10.8±7.9
Empty DL-9 after dialysis	141±19.5	−22.2±7.1
Purified 4HT-DL-9 liposomes, 5 min heating	144±46	−23.9±7.6
Purified 4HT-DL-9 liposomes, 1 h heating	144±28.5	−10.6±6.3

The diameter (mean ± Pdl width nm) and the zeta potential (mean ± zeta deviation mV) were measured before and after dialysis for empty liposomes and after gel filtration purification of 4HT-DL-9 liposomes following either 5 min or 1 h heating. Results are the mean (± SD) of at least 3 different measurements on 3 different preparations.

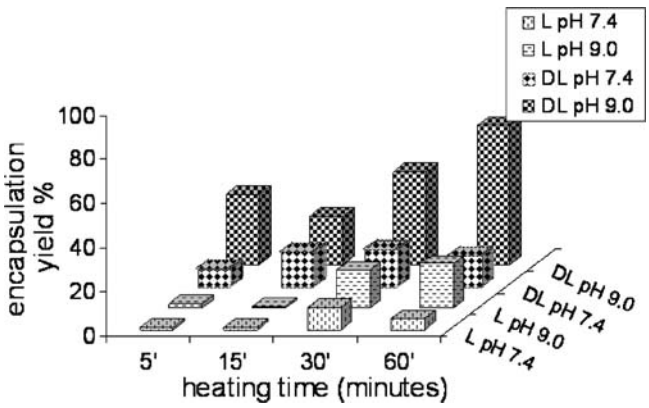

Fig. 1. Drug loading efficiency of the four groups of pH-gradient liposomes. The encapsulation yields for the different pH-gradient 4HT liposomes (determined from the AUC from the HPLC analyses) are shown. Results are expressed as the mean (± SD) of three measures from three different preparations of the four 4HT-loaded formulations.

contrast, ePG appeared to enhance the incorporation of the drug, by strengthening the interactions between the encapsulated drug and the negative charges of ePG. All formulations incorporated a high amount of 4HT, from 324 μg/38 mg lipids (equivalent to 0.8 mM 4HT) up to 435 μg/ 40 mg lipids (corresponding to 1.1 mM 4HT) for the formulations with the greatest load.

pH-gradient Liposomes

Each of the four pH-gradient L and DL liposomes displayed various capacities to encapsulate 4HT (Fig. 1). None of the formulations reached maximum loading capacity even after 15 min of heating at pH 7.4. Liposomes with an external pH 7.4 needed 30 min of heating to reach the maximal drug encapsulation, and increasing the pH to 9 led to enhanced 4HT loading even at 60 min heating. When the external pH was changed to 9, the drug loading capacity was increased, with a greater drug encapsulation observed for liposomes containing twice the amount of lipids (DL-9). This is explained by the fact that increased pH confers a neutral charge to 4HT, which can then easily cross the lipid barrier and accumulate in the core of liposomes. The acidic pH of the inner core of the liposome allows 4HT to remain ionized, impeding its release across the lipid membrane. The amount of 4HT encapsulated in DL-9 pH-gradient liposomes reached 306 μg/30 mg lipids (corresponding to 0.8 mM).

Release Kinetics of 4HT and Subsequent Biological Activity of the Drug

MELN cells were used to investigate 4HT leak from the liposomes and to check whether the encapsulated molecule retained its biological activity. In this breast cancer cell line, 4HT inhibits E_2-induced transcription both through a dose- and time-dependent process (48). Moreover, this cell system reflects much better the *in vivo* situation than the physical dialysis methods generally employed to measure the release of an entrapped drug. Indeed, following i.v. injection, the 4HT-loaded nanocarriers are in a biological environment which can be mimicked by the cell culture medium. We then measured the luciferase activity in MELN cells exposed to free or encapsulated 4HT in inserts for various times in the presence of 0.1 nM E_2. Previous data established that this E_2 concentration gives the maximal luciferase activity in these cells (50). The system was designed to avoid direct contact of cells with liposomes, allowing cell contact only with the drug released from the colloidal system. Free 4HT inhibited E_2-induced luciferase transcription by almost 75% over the first hour, and this level of inhibition remained constant at 24 h, indicating the maximum inhibition obtainable in these conditions (Fig. 2). Whatever the conventional liposomal formulation, the same inhibitory potential as that displayed for free 4HT was obtained, in agreement with a rapid release of the drug from these nanocarriers (Figs. 2A and B). We previously showed that empty liposomes do not have the capacity to inhibit transcription (33).

By contrast, the dose-response inhibition curve obtained for 4HT released from pH-gradient DL-9 liposomes showed that not more than 50% inhibition was obtained at 6 h. The curve then remained stable until 48 h, suggesting that part of the drug was still encapsulated (Fig. 2C). Empty DL-9 liposomes had no effect on transcriptional inhibition. Similarly, the kinetic of drug release was monitored, comparing the inhibitory effect on transcription of free drug to that of a physical mixture of uncharged DL-9 liposomes and free 4HT (Fig. 2D). No difference in luciferase expression between the two systems was observed. These data from Fig. 2D demonstrate that 4HT added to empty liposomes behaves differently than encapsulated 4HT, strongly confirming the importance of a colloidal system surrounding the active molecule to prevent its fast release. Since 4HT-DL-9 liposomes displayed the greatest capacity for retaining 4HT, this formulation was assayed in *in vivo* experiments.

Enhanced Anti-proliferative Activity of 4HT pH-gradient Liposomes

Flow cytometry analysis following exposure of MCF-7 breast cancer cells to either free 4HT or liposome-loaded 4HT revealed an increase of cell number in the G0/G1 phase of the cell cycle in both cases, with a pronounced marked effect with 4HT pH-gradient liposomes (Table IIIA) at 72 h concomitantly with a decreased number of cells in G2/M. This indicated a 4HT-mediated arrest at the G1/S check point and a blockade of cell proliferation as observed previously (53,54). Moreover, a tendency to increase the number of cells in sub-G1 was noticed. In RPMI 8226 MM cells, 4HT-DL-9 liposomes also increased the number of cells in sub-G1, depending on time and dose (Table IIIB). This effect was found at a lower extent after treatment with free 4HT. This supports a greater extent of cellular uptake of the liposome-encapsulated AE and may reflect an enhanced reticulum endothelium-mediated caspase apoptosis process as indicated previously (18). These results are in agreement with the enhancement of the cellular capture of the other AE RU once entrapped in liposomes, a process also reported to bypass the extrusion capacity of Pgps (33).

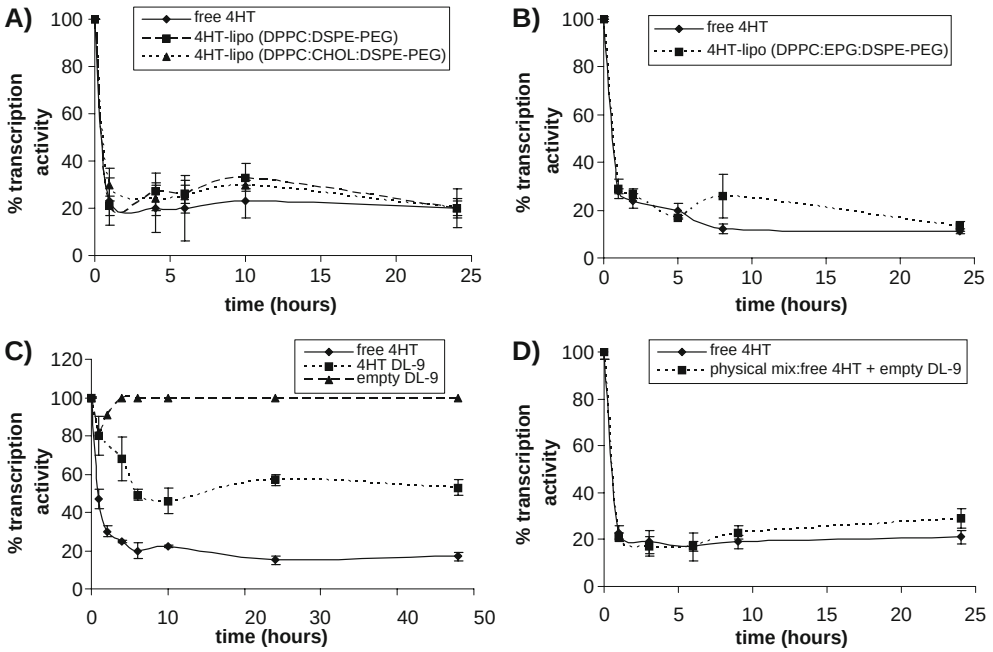

Fig. 2. Inhibition of estradiol-induced transcription by 4HT loaded conventional and pH-gradient liposomes. MELN cells were exposed or not to either free (all four panels) or encapsulated 4HT (10 nM) from conventional liposomes (panels A and B) and from pH-gradient DL-9 liposomes (panel C) added to inserts in the culture dishes in the presence of 0.1 nM estradiol (E_2) supplemented medium. In panel D, a physical mixture of 4HT at 10 nM and of empty DL-9 liposomes was added to the culture medium. Results show the percentage of luciferase inhibition relative to the activity in E_2-treated cells in the absence of competitor (100% activity). Each point represents the mean value (± SD) of three measurements.

Cell Viability

The MTT test was carried out for the pH-gradient liposomes with double lipid content DL-9 (Fig. 3). Empty liposomes revealed no toxicity on both MCF-7 (Fig. 3A and B) and RPMI8226 (Fig. 3C and D) cells, in agreement with flow cytometry results. In the case of free 4HT, the viability of MCF-7 cells was affected only at 10 μM at 48 h and at lower concentrations at 72 h (starting at 0.1 μM). Ten to 15% of MCF-7 remained viable at 10 μM free 4HT after 72 h. In these cells, encapsulated 4HT in DL-9 liposomes was less efficient than free 4HT at concentrations between 0.1 and 1 μM. This

Table III. Influence of Free and Encapsulated 4HT on Cell Cycle Distribution of MCF-7 and RPMI8226 Cells

	Sub G1		G0/G1		S		G2/M	
A. MCF-7								
	48 h	72 h	48 h	72 h	48 h	72 h	48 h	72 h
NT (EtOH)	2.3	2.2	68.4	73.9	16.6	13.4	15	12.7
Empty DL-9 1	2.1	3.2	65.9	74	18.4	14.4	15.7	11.6
Empty DL-9 10	3.2	3.6	69.5	74.8	18.2	14.2	7.3	5.9
4HT 1	2.2	3.1	68.8	78.8	17.9	13.8	13.8	9.1
4HT 10	2.9	3.9	70.7	78.1	15.6	12	10.7	8.1
4HT-DL-9 1	4.8	4.9	69.5	78	17.3	12.7	13.2	9
4HT-DL-9 10	5.4	6.6	78.4	87.4	13.4	8.6	8.4	4
B. RPMI8226								
	24 h	48 h	24 h	48 h	24 h	48 h	24 h	48 h
NT (EtOH)	5.2	12.4	18.6	46.5	58.6	34.2	22.8	19.3
Empty DL-9 1	5.2	12.3	21	47.1	60.4	31.7	18.5	21.1
Empty DL-9 10	5.1	12.6	20.4	48.5	61.6	34.9	17.9	16.6
4HT 1	4.8	13.3	19.4	49	55.7	31.7	24.8	19.2
4HT 10	10.4	15.4	20	49	50.4	46.7	29.5	16
4HT-DL-9 1	7.5	16.9	25	49	48.3	37.2	25.5	13.5
4HT-DL-9 10	8.2	19.6	27.6	52	50.4	39	22	9

MCF-7 (A) and RPMI8226 (B) cells were analyzed by flow cytometry as described in Material and Methods. Numbers indicate the percentage of cells in the phases of the cycle after exposure to free (4HT-1 and 4HT-10) or encapsulated 4HT in pH-gradient liposomes at 1 and 10 μM (4HT-DL-9 1 and 4HT-DL-9 10, respectively) during 48 and 72 h for MCF-7 cells and 24 and 48 h for RPMI cells. The influence on cell cycle of empty DL-9 liposomes at a concentration equivalent to that of 4HT-loaded loposomes was also measured (Empty DL-1 and Empty DL-9 10, respectively). The percentage of cells in sub-G1 is indicated. Results are representative of two experiments performed with two different sets of DL-9 liposomes.

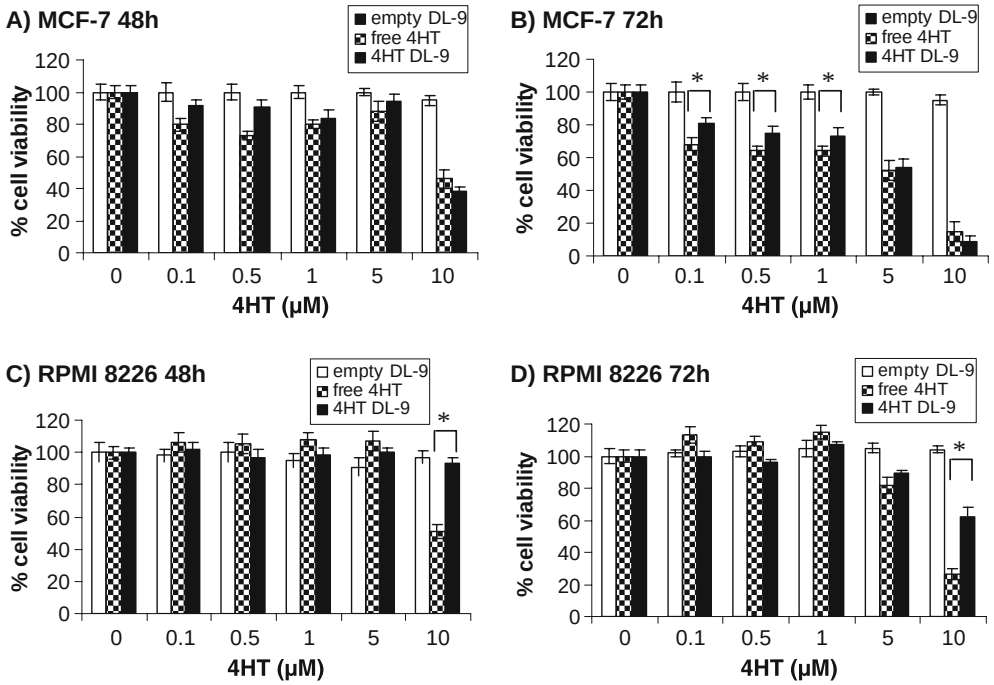

Fig. 3. Viability of MCF-7 breast cancer cells and RPMI8226 MM cells after exposure to DL-9 liposomes. Cells were exposed to free 4HT and 4HT-DL-9 liposomes at various 4HT concentrations or to unloaded liposomes at equivalent lipid concentrations for 48 (A and C) or 72 (B and D) hours. The number of remaining living cells was quantified by the MTT test. Each experiment was repeated eight times on three independent DL-9 liposome preparations. Results are presented as means (± SD), with * $p<0.05$ (Student t test).

may be explained by a slow release of 4HT from liposomes giving at each time a 4HT concentration inferior to that of the free 4HT. At higher concentrations, the difference between free and encapsulated 4HT was not visible due to the saturation of the system by such high AE concentrations. Both free and encapsulated 4HT at 10μM were similarly efficient to reduce MCF-7 cell viability (Fig. 3B).

On the contrary, in RPMI8226 cells, the cell viability at 48 and 72 h was always less affected by 4HT-DL-9 liposomes than by free 4HT. This may be again the consequence of a slow 4HT release from pH-gradient liposomes. The fact that 4HT becomes toxic for MM cells at 10μM correlates with previous data obtained by us and others (15,17,55). Nevertheless, results from flow cytometry and cell viability could seem contradictory, since the former indicated a potency of cell-death induction by encapsulated 4HT greater than free 4HT, while the latter revealed a reverse behavior. The weaker activity of 4HT-DL-9 liposomes in the MTT test is explainable, besides slow 4HT release from liposomes, by the capacity of 4HT to inhibit Pgps favoring tetrazolium salt accumulation leading to artificially increased number of viable cells. In fact, it has already been demonstrated that Tam enhances intracellular deposition of natural product chemotherapy in human cell lines by inhibition of Pgps (56,57).

Tumor Growth Evolution

As shown in Fig. 4, MM tumors from mice injected with 4HT-containing DL-9 liposomes showed a significant weaker growth than untreated mice after 6 weeks of treatment. The evolution of tumors from mice injected with the corresponding concentration of empty DL-9 liposomes was strictly equivalent to that of untreated mice (super imposable curves, not shown), indicating a lack of intrinsic anti-tumor activity of these empty liposomes. Injection of free 4HT at equivalent concentration to that of encapsulated 4HT in DL-9 liposomes was performed. However, 4HT is not soluble at concentrations above 10μM, and we observed crystallized material in the stock solution of 4HT in 5% glucose. Then, even if the evolution curve of the tumors from mice injected in these conditions is super imposable to that of the controls, as already observed in other *in vivo* experiments performed with MCF-7 xenografts at similar free 4HT concentrations (31), the exact concentration of injected 4HT remains uncertain.

Organs (liver, lung, spleen) from mice injected or not with DL-9 liposomes were removed and fixed, and slices were stained with HES, indicating a preserved integrity of the tissue structure (not shown) in agreement with no toxicity of the liposomes in other tissues than the tumor. Immunohistochemistry studies performed on tumor slices (Fig. 4B) demonstrated a strong decrease of the proliferative index Ki67 labeling in cell nuclei of tumors from 4HT-DL-9-treated mice. In correlation with *in vitro* results, which showed an increase number of cells in subG1 after 4HT treatment (both free and encapsulated), a strong labeling of activated caspase-3 was observed. This is accompanied by the normalization of tumor vasculature and the decrease of the number and the size of vessels as demonstrated by CD34 labeling (Fig. 4B).

Biodistribution

As shown in Fig. 5A, after 1 h treatment with free and conventional 4HT-loaded liposomes, a major fraction of ^{3}H-4HT was recovered in the liver and the lung, indicating a fast capture by these organs. A small amount of 4HT was found in

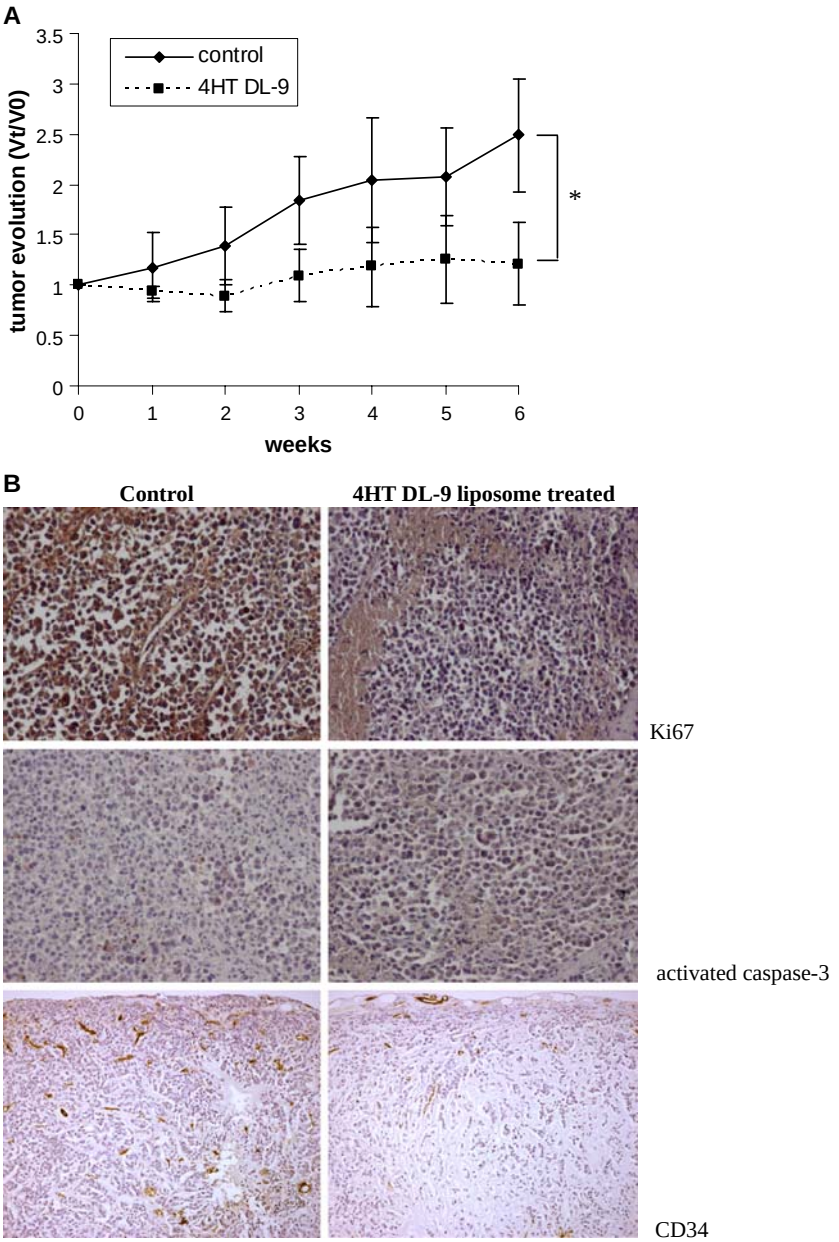

Fig. 4. *In vivo* antitumor efficiency of 4HT-DL-9 liposomes. Mice (8 weeks old; 6 per group) were subcutaneously injected with RPMI 8226 cells as described in Material and Methods. After tumor developed at the site of injection (4–5 weeks) mice were biweekly i.v.-injected with 200µL of 4HT-DL-9 liposomes (■) (total 4HT concentration 4 mg/kg/week) or not (control) (♦) or with empty DL-9 liposomes (not shown, same curve as the controls). Tumor volume was measured each week and the volume Vt calculated as described in Material and Methods during 6 weeks. Panel A represents the evolution of the tumors (mean ± SD of double blind measures) as compared to volumes of the tumors at $t=0$ (V0). A significant difference between the two curves was found * $p<0.05$ (ANOVA test). In panel B, immunohisto-chemical analysis of Ki-67, cleaved caspase 3 and CD34 are shown. Images (200X for Ki67 and caspase-3, 100X for CD34) are representative of three different similarly treated tumors.

the tumor and in the uterus. These data indicated a comparable biodistribution of the AE between free 4HT and 4HT from conventional liposomes, except that 4HT-containing liposomes revealed a tendency to accumulate also in the spleen (Fig. 5A). This is in favor of a typical increased immunological recognition of nanocarriers by this organ (58). The 4HT-pH-gradient liposomes do not have the same behavior, although the radioactivity was principally concentrated in the spleen but not in the lung and the liver. At 24 h, a small amount of 4HT, whether free or encapsulated in conventional liposomes, was still captured by the liver and the lung, and again a small amount (less than 9% of the total radioactivity) by the tumor. On the contrary, 4HT-DL-9 liposomes, mainly accumulated in the tumor (37% of the total radioactivity measured). At this time, the total radioactivity of the five organs represented 17% and 19% of the radioactivity measured at 1 h for free 4HT and 4HT-

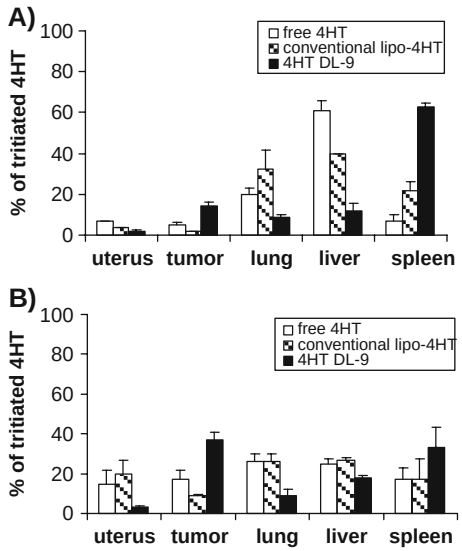

Fig. 5. Biodistribution of 4HT in xenografts. Mice bearing RPMI8226 tumors (3 per group) as in Fig. 4 were injected with 10^6cpm of free tritiated 4HT or entrapped in conventional liposomes or in DL-9 liposomes. After 1 h (panel A) and 24 h (panel B), organs were removed and treated as described in Materials and Methods. Note that only free radioactive 4HT diluted in 5% glucose was injected, while isotopically diluted tritiated 4HT-loaded liposomes were injected (see Materials and Methods for details). Results are expressed as the percentage of radioactivity (mean ± SD) measured in triplicate in each organ relative to the total radioactivity measured in the five organs.

loaded liposomes, respectively. Importantly, the total radioactivity measured at 24 h in the organs from mice injected with 4HT-DL-9 liposomes represented 46% of that measured at 1 h (Fig. 5B). Taken together, these results indicate an elevated clearance of free 4HT and of 4HT-conventional liposomes, leading to a low 4HT uptake by the tumor and a better biodistribution of the 4HT from DL-9 liposomes, resulting in higher 4HT accumulation in the target tissue.

DISCUSSION

Tam is the most widely used antiestrogen for the therapy of premenopausal and postmenopausal women with hormone-dependent breast cancer (59). A lot of nanocarriers using nanospheres and nanocapsules for the encapsulation of Tam (or its orally available precursors like 4HT) were synthesized in the past, but only a small number of liposomal nanocarriers incorporating Tam were realized (36,60). Most of the previously described 4HT-containing liposomes have been evaluated in breast cancer models, but they were not able to retain high amount of drug. For example, only 1.09 μM 4HT was measured to be encapsulated in liposomes composed of lecithin/Chol/dicetylphosphate (35) and only up to 45 μM 4HT were incorporated in liposomes made of ox-brain phospholipids dispersed in aqueous medium (61). Our goal was to realize a liposomal formulation capable of high 4HT encapsulation with a prolonged blood circulation time *in vivo* in order to reach MM cells. The amount of 4HT incorporated in the pH-gradient liposomes described in this work is thus more than one order of magnitude higher than that incorporated in the previously described liposomal systems.

We compared various pegylated liposomes produced through different methods to optimize the retention of 4HT. Most of them had a size compatible with a prolonged blood circulation time once i.v. injected and were able to incorporate the drug at a high rate. However, conventional liposomes revealed a very fast release of the incorporated drug both *in vitro* and *in vivo*. The DL-9 liposomes we have later developed were stable and incorporated high amounts of 4HT. Such a high 4HT concentration is impossible to attain in the absence of an efficient nanocarrier because of its weak solubility. The kinetics of 4HT released from 4HT-DL-9 liposomes (Fig. 2) showed an inhibitory capacity of 4HT weaker than that of free 4HT, attributable to a burst effect during the first 6 h of the period of cell incubation. After 6 h, the system seemed to retain an important part of the encapsulated drug. This behavior could be explained if we consider two populations of encapsulated 4HT. One fraction not protonated because of the external pH of 9.0 interacts with the lipid bilayer and tends to remain at the surface of the liposomes. This population will easily escape from the system and gives the burst effect observed during the first 6 h, still with a weaker extent than 4HT released from conventional liposomes. The faster release of 4HT from conventional liposomes is explained by a weaker interaction between their lipids and the drug, in this case positively charged because of the external pH of 7.4. The second population of incorporated 4HT (also 50% of the total encapsulated drug) does not seem to be released in the conditions used in the Fig. 2 experiment, because it is localized inside the core of liposomes where the pH is 5.1. At such a pH, 4HT is also protonated and incapable of crossing through the lipid bilayer. Importantly, this does not occur *in vivo* because the 4HT-DL-9 liposomes release both the adsorbed and the encapsulated 4HT inside the tumor cells following their endocytosis.

The bio-distribution of 4HT released from DL-9 liposomes compared with that of 4HT released from conventional liposomes showed dramatic differences. The amount of 4HT captured by the tumor was higher in the case of pH-gradient liposomes than in the case of conventional liposomes, already after 1 h. Since both these nanocarriers are pegylated and then supposed to have a prolonged circulation time, the differences in the accumulation of 4HT must be attributable to the longer retention of 4HT in DL-9 liposomes than in conventional liposomes. The proportion of 4HT recovered in the tumor at 24 h treated with DL-9 liposomes remained constant, supporting accumulation of 4HT-DL-9 liposomes at the tumor site capillaries.

The *in vivo* efficiency of a formulation to act as a potent therapeutic is a prerequisite to its clinical evaluation. We assayed the antitumor activity of the formulations described here in a commonly used model (33,62,63) which preserves neo-angiogenesis characteristics necessary for the development of the disease (62). Similar to the effects of 4HT which arrest RPMI8226 cell proliferation *in vitro*, *in vivo* experiments showed that 4HT-DL-9 liposomes arrest tumor growth (Fig. 4). This was confirmed by a decrease of Ki67 labeling concomitantly with an increase of activated caspase 3 revealing enhancement of cell death. A normalization of the vasculature was also noticed as revealed by the decrease of the number and size of tumor capillaries. This is in agreement with the fact that AEs, like 2-methoxy estradiol (62,64) inhibit the synthesis and secretion of Vascular Endothelial Growth Factor (VEGF) not

only in MCF-7 and MDA-MB-231 breast tumors (65,66), but also in RPMI8226 cells (31,33). Despite the fact that the xenograft model used here does not reflect the human pathology which affects bone marrow in priority, it is tempting to speculate that this 4HT-DL-9 pH gradient liposomal formulation may confer to AE a distinct therapeutic advantage not only for breast cancer but also for MM treatment. It constitutes a new tool helpful for the delivery of high concentration of 4HT. VEGF is the major actor of vascular growth in MM, since it triggers growth, survival and migration of MM cells (67). As a consequence, deregulation of VEGF as well as other factors affecting the vasculature network may provide a potent therapeutic approach, whether alone or in combination with other drugs such as the classical melphalan (68) or proteasome inhibitors (69,70), to overcome resistance to therapies and thereby improve patient outcome. Such an antitumor activity combined with the 4HT-triggered cell death of MM obtained with liposomes loaded with high dose of AE, whether 4HT (this work) or RU58668 (33), could be of clinical interest.

Nevertheless, the involvement of the ER from MM cells in the antitumor effects induced by 4HT is still the matter of debate because the 4HT-induced inhibition of the classical ER activity, due to the high affinity of ER for 4HT (Kd~ 1 nM), occurs at lower 4HT concentration than 10 μM. Indeed, in breast cancer cells, 4HT blocks proliferation in the G0/G1 phase of the cell cycle already at 10 nM (71), and this effect is reversed by a 10-fold excess of AE (72) and is strictly ER specific. By contrast, in MM cells, the arrest of cell cycle occurs at 5 to 10 μM 4HT, and, despite the presence of ER, we wondered if this effect is mediated only through inhibition of ER activity. Others have proposed that such an elevated concentration of AE could result in cell membrane perturbation, including multidrug-resistance-related processes (73), or in the induction cell death and autophagy (13). To date, no data exist to explain the molecular mechanism(s) by which AEs induce apoptosis in MM cells.

CONCLUSION

The 4HT pH-gradient DL-9 liposomes may represent a new framework for the delivery of 4HT by i.v. for the treatment of hormone-dependent breast cancers and also for MM. This pathology is characterized by accumulation of malignant plasma cells in the bone marrow milieu. In the case of MM, giving the 4HT formulation by i.v. would be directly in the vicinity of the tumor cells. That may allow a better bio-availability of the drug because no biological barriers have to be crossed. In the case of hormone-dependent breast cancer, Tam is given orally at a relatively high dose (20 mg/day) over a period never exceeding 5 years. The use of 4HT-DL-9 liposomes injected by i.v. could be of therapeutic advantage by avoiding the adsorption phenomenon and eliminating the first pass metabolism through the liver typical of orally administrated drug. Increasing the bio-availability at the tumor level and reducing the efficient dose will result in a better outcome for patients.

ACKNOWLEDGMENTS

We thank Besins Iscovesco for the generous gift of 4HT, J. Bignon for FACS analyses and M. Pons and P. Ballaguer for the gift of MELN cells. This work was supported by the Ligue Nationale contre le Cancer through a fellowship offered to G.U. and financial support was provided to J-M. R from the Comités du Cher, de l'Indre et des Hauts de Seine of the Ligue Nationale contre le Cancer.

REFERENCES

1. Fisher B, Costantino JP, Wickerham DL, Redmond CK, Kavanah M, Cronin WM, *et al.* Tamoxifen for prevention of breast cancer: report of the national surgical adjuvant breast and bowel project P-1 study. J Natl Cancer Inst. 1998;90:1371–88.
2. Jordan VC, Jordan VC. Tamoxifen (ICI46,474) as a targeted therapy to treat and prevent breast cancer. Br J Pharmacol. 2006;147(Suppl 1):S269–76.
3. Ellis CA, Vos MD, Wickline M, Riley C, Vallecorsa T, Telford WG, *et al.* Tamoxifen and the farnesyl transferase inhibitor FTI-277 synergize to inhibit growth in estrogen receptor-positive breast tumor cell lines. Breast Cancer Res Treat. 2003;78:59–67.
4. Obrero M, Yu DV, Shapiro DJ. Estrogen receptor-dependent and estrogen receptor-independent pathways for tamoxifen and 4-hydroxytamoxifen-induced programmed cell death. J Biol Chem. 2002;277:45695–703.
5. Zheng A, Kallio A, Harkonen P. Tamoxifen-induced rapid death of MCF-7 breast cancer cells is mediated via extracellularly signal-regulated kinase signaling and can be abrogated by estrogen. Endocrinology. 2007;148:2764–77.
6. Dutertreand M, Smith CL. Molecular mechanisms of selective estrogen receptor modulator (SERM) action. J Pharmacol Exp Ther. 2000;295:431–7.
7. MacGregor JI, Jordan VC. Basic guide to the mechanisms of antiestrogen action. Pharmacol Rev. 1998;50:151–96.
8. Mangelsdorf DJ, Thummel C, Beato M, Herrlich P, Schutz G, Umesono K, *et al.* The nuclear receptor superfamily: the second decade. Cell. 1995;83:835–9.
9. Effects of chemotherapy and hormonal therapy for early breast cancer on recurrence and 15-year survival: an overview of the randomised trials. Lancet 2005; 365:1687-717.
10. Rossouw JE, Anderson GL, Prentice RL, LaCroix AZ, Kooperberg C, Stefanick ML, *et al.* Risks and benefits of estrogen plus progestin in healthy postmenopausal women: principal results from the women's health initiative randomized controlled trial. JAMA. 2002;288:321–33.
11. Goldenberg GJ, Froese EK. Drug and hormone sensitivity of estrogen receptor-positive and -negative human breast cancer cells *in vitro*. Cancer Res. 1982;42:5147–51.
12. Gelmann EP. Tamoxifen for the treatment of malignancies other than breast and endometrial carcinoma. Semin Oncol. 1997;24: S1-65–70.
13. de Medina P, Payre B, Boubekeur N, Bertrand-Michel J, Terce F, Silvente-Poirot S, *et al.* Ligands of the antiestrogen-binding site induce active cell death and autophagy in human breast cancer cells through the modulation of cholesterol metabolism. Cell Death Differ. 2009.
14. Sjak-Shie NN, Vescio RA, Berenson JR. Recent advances in multiple myeloma. Curr Opin Hematol. 2000;7:241–6.
15. Treon SP, Teoh G, Urashima M, Ogata A, Chauhan D, Webb IJ, *et al.* Anti-estrogens induce apoptosis of multiple myeloma cells. Blood. 1998;92:1749–57.
16. Otsuki T, Yamada O, Kurebayashi J, Moriya T, Sakaguchi H, Kunisue H, *et al.* Estrogen receptors in human myeloma cells. Cancer Res. 2001;60:1434–41.
17. Gauduchon J, Gouilleux F, Maillard S, Marsaud V, Renoir JM, Sola B. The 4-hydroxytamoxifen inhibits proliferation of multiple myeloma cells *in vitro* and *in vivo* through down-regulation of c-Myc, up-regulation of p27Kip1 and modulation of Bcl-2 family members. Clin Cancer Res. 2005;11:2345–54.
18. Gauduchon J, Seguin A, Marsaud V, Clay D, Renoir JM, Sola B. Pure antiestrogen-induced G1-arrest in myeloma cells results from the reduced kinase activity of cyclin D3/CDK6 complexes whereas apoptosis is mediated by endoplasmic reticulum-dependent caspases. Int J Cancer. 2008;122:2130–41.

19. Sola B, Renoir JM. Estrogenic or antiestrogenic therapies for multiple myeloma? Mol Cancer. 2007;6:59.
20. Olivier S, Close P, Castermans E, de Leval L, Tabruyn S, Chariot A, *et al.* Raloxifene-induced myeloma cell apoptosis: a study of nuclear factor-kappaB inhibition and gene expression signature. Mol Pharmacol. 2006;69:1615–23.
21. Prall OW, Rogan EM, Sutherland RL. Estrogen regulation of cell cycle progression in breast cancer cells. J Steroid Biochem Mol Biol. 1998;65:169–74.
22. Clarke R, Leonessa F, Welch JN, Skaar TC. Cellular and molecular pharmacology of antiestrogen action and resistance. Pharmacol Rev. 2001;53:25–71.
23. Rochefort H, Borgna JL. Differences between oestrogen receptor activation by oestrogen and antioestrogen. Nature. 1981;292:257–9.
24. Katzenellenbogen BS, Montano MM, Le Goff P, Schodin DJ, Kraus WL, Bhardwaj B, *et al.* Antiestrogens: mechanisms and actions in target cells. J Steroid Biochem Mol Biol. 1995;53:387–93.
25. Brigger I, Chaminade P, Marsaud V, Appel M, Besnard M, Gurny R, *et al.* Tamoxifen encapsulation within polyethylene glycol-coated nanospheres. A new antiestrogen formulation. Int J Pharm. 2001;214:37–42.
26. Chawla JS, Amiji MM. Biodegradable poly(epsilon -caprolactone) nanoparticles for tumor-targeted delivery of tamoxifen. Int J Pharm. 2002;249:127–38.
27. Devalapally H, Duan Z, Seiden MV, Amiji MM. Modulation of drug resistance in ovarian adenocarcinoma by enhancing intracellular ceramide using tamoxifen-loaded biodegradable polymeric nanoparticles. Clin Cancer Res. 2008;14:3193–203.
28. Shenoy D, Little S, Langer R, Amiji M. Poly(ethylene oxide)-modified poly(beta-amino ester) nanoparticles as a pH-sensitive system for tumor-targeted delivery of hydrophobic drugs: part 2. *In vivo* distribution and tumor localization studies. Pharm Res. 2005;22:2107–14.
29. Memisoglu-Bilensoy E, Vural I, Bochot A, Renoir JM, Duchene D, Hincal AA. Tamoxifen citrate loaded amphiphilic beta-cyclodextrin nanoparticles: *in vitro* characterization and cytotoxicity. J Control Release. 2005;104:489–96.
30. Hu FX, Neoh KG, Kang ET. Synthesis and *in vitro* anti-cancer evaluation of tamoxifen-loaded magnetite/PLLA composite nanoparticles. Biomaterials. 2006;27:5725–33.
31. Renoir JM, Stella B, Ameller T, Connault E, Opolon P, Marsaud V. Improved anti-tumoral capacity of mixed and pure anti-oestrogens in breast cancer cell xenografts after their administration by entrapment in colloidal nanosystems. J Steroid Biochem Mol Biol. 2006;102:114–27.
32. Ameller T, Marsaud V, Legrand P, Gref R, Barratt G, Renoir JM. Polyester-poly(ethylene glycol) nanoparticles loaded with the pure antiestrogen RU 58668: physicochemical and opsonization properties. Pharm Res. 2003;20:1063–70.
33. Maillard S, Gauduchon J, Marsaud V, Gouilleux F, Connault E, Opolon P, *et al.* Improved antitumoral properties of pure antiestrogen RU 58668-loaded liposomes in multiple myeloma. J Steroid Biochem Mol Biol. 2006;100:67–78.
34. Bhatia A, Kumar R, Katare OP. Tamoxifen in topical liposomes: development, characterization and *in-vitro* evaluation. J Pharm Pharm Sci. 2004;7:252–9.
35. Zeisig R, Teppke AD, Behrens D, Fichtner I. Liposomal 4-hydroxy-tamoxifen: effect on cellular uptake and resulting cytotoxicity in drug resistant breast cancer cells *in vitro*. Breast Cancer Res Treat. 2004;87:245–54.
36. Zeisig R, Ruckerl D, Fichtner I. Reduction of tamoxifen resistance in human breast carcinomas by tamoxifen-containing liposomes *in vivo*. Anticancer Drugs. 2004;15:707–14.
37. Daoud-Mahammed S, Couvreur P, Bouchemal K, Cheron M, Lebas G, Amiel C, *et al.* Cyclodextrin and Polysaccharide-Based Nanogels: Entrapment of Two Hydrophobic Molecules, Benzophenone and Tamoxifen. Biomacromolecules 2009.
38. Lasic DD, Frederik PM, Stuart MC, Barenholz Y, McIntosh TJ. Gelation of liposome interior. A novel method for drug encapsulation. FEBS Lett. 1992;312:255–8.
39. Haran G, Cohen R, Bar LK, Barenholz Y. Transmembrane ammonium sulfate gradients in liposomes produce efficient and stable entrapment of amphipathic weak bases. Biochim Biophys Acta. 1993;1151:201–15.
40. Harrigan PR, Wong KF, Redelmeier TE, Wheeler JJ, Cullis PR. Accumulation of doxorubicin and other lipophilic amines into large unilamellar vesicles in response to transmembrane pH gradients. Biochim Biophys Acta. 1993;1149:329–38.
41. Celano M, Calvagno MG, Bulotta S, Paolino D, Arturi F, Rotiroti D, *et al.* Cytotoxic effects of gemcitabine-loaded liposomes in human anaplastic thyroid carcinoma cells. BMC Cancer. 2004;4:63.
42. Stella B, Arpicco S, Rocco F, Marsaud V, Renoir JM, Cattel L, *et al.* Encapsulation of gemcitabine lipophilic derivatives into polycyanoacrylate nanospheres and nanocapsules. Int J Pharm. 2007;344:71–7.
43. Abraham SA, Edwards K, Karlsson G, Hudon N, Mayer LD, Bally MB. An evaluation of transmembrane ion gradient-mediated encapsulation of topotecan within liposomes. J Control Release. 2004;96:449–61.
44. Abraham SA, McKenzie C, Masin D, Ng R, Harasym TO, Mayer LD, *et al. In vitro* and *in vivo* characterization of doxorubicin and vincristine coencapsulated within liposomes through use of transition metal ion complexation and pH gradient loading. Clin Cancer Res. 2004;10:728–38.
45. Chemin C, Pean JM, Bourgaux C, Pabst G, Wuthrich P, Couvreur P, *et al.* Supramolecular organization of S12363-liposomes prepared with two different remote loading processes. Biochim Biophys Acta. 2009;1788:926–35.
46. Ramsay E, Alnajim J, Anantha M, Zastre J, Yan H, Webb M, *et al.* A novel liposomal irinotecan formulation with significant anti-tumour activity: use of the divalent cation ionophore A23187 and copper-containing liposomes to improve drug retention. Eur J Pharm Biopharm. 2008;68:607–17.
47. Pons M, Gagne D, Nicolas JC, Mehtali M. A new cellular model of response to estrogens: a bioluminescent test to characterize (anti) estrogen molecules. Biotechniques. 1990;9:450–9.
48. Balaguer P, Francois F, Comunale F, Fenet H, Boussioux AM, Pons M, *et al.* Reporter cell lines to study the estrogenic effects of xenoestrogens. Sci Total Environ. 1999;233:47–56.
49. Maillard S, Ameller T, Gauduchon J, Gougelet A, Gouilleux F, Legrand P, *et al.* Innovative drug delivery nanosystems improve the anti-tumor activity *in vitro* and *in vivo* of anti-estrogens in human breast cancer and multiple myeloma. J Steroid Biochem Mol Biol. 2005;94:111–21.
50. Marsaud V, Gougelet A, Maillard S, Renoir JM. Various phosphorylation pathways, depending on agonist and antagonist binding to endogenous estrogen receptor alpha (ERalpha), differentially affect ERalpha extractability, proteasome-mediated stability, and transcriptional activity in human breast cancer cells. Mol Endocrinol. 2003;17:2013–27.
51. Moghimi SM, Szebeni J. Stealth liposomes and long circulating nanoparticles: critical issues in pharmacokinetics, opsonization and protein-binding properties. Prog Lipid Res. 2003;42:463–78.
52. Allen TM, Cullis PR. Drug delivery systems: entering the mainstream. Science. 2004;303:1818–22.
53. Watts CK, Brady A, Sarcevic B, deFazio A, Musgrove EA, Sutherland RL. Antiestrogen inhibition of cell cycle progression in breast cancer cells in associated with inhibition of cyclin-dependent kinase activity and decreased retinoblastoma protein phosphorylation. Mol Endocrinol. 1995;9:1804–13.
54. Cariou S, Donovan JC, Flanagan WM, Milic A, Bhattacharya N, Slingerland JM. Down-regulation of p21WAF1/CIP1 or p27Kip1 abrogates antiestrogen-mediated cell cycle arrest in human breast cancer cells. Proc Natl Acad Sci USA. 2000;97:9042–6.
55. Otsuki T, Yamada O, Kurebayashi J, Moriya T, Sakaguchi H, Kunisue H, *et al.* Estrogen receptors in human myeloma cells. Cancer Res. 2000;60:1434–41.
56. Berman E, Adams M, Duigou-Osterndorf R, Godfrey L, Clarkson B, Andreeff M. Effect of tamoxifen on cell lines displaying the multidrug-resistant phenotype. Blood. 1991;77:818–25.
57. Trump DL, Smith DC, Ellis PG, Rogers MP, Schold SC, Winer EP, *et al.* High-dose oral tamoxifen, a potential multidrug-resistance-reversal agent: phase I trial in combination with vinblastine. J Natl Cancer Inst. 1992;84:1811–6.
58. Demoy M, Gibaud S, Andreux JP, Weingarten C, Gouritin B, Couvreur P. Splenic trapping of nanoparticles: complementary approaches for *in situ* studies. Pharm Res. 1997;14:463–8.

59. Osborne CK. Tamoxifen in the treatment of breast cancer. N Engl J Med. 1998;339:1609–18.
60. Bhatia A, Bhushan S, Singh B, Katare OP. Studies on Tamoxifen Encapsulated in Lipid Vesicles: Effect on the Growth of Human Breast Cancer MCF-7 Cells. J Liposome Res. 2008;1-6.
61. Wiseman H, Quinn P, Halliwell B. Tamoxifen and related compounds decrease membrane fluidity in liposomes. Mechanism for the antioxidant action of tamoxifen and relevance to its anticancer and cardioprotective actions? FEBS Lett. 1993;330:53–6.
62. Chauhan D, Catley L, Hideshima T, Li G, Leblanc R, Gupta D, *et al.* 2-Methoxyestradiol overcomes drug resistance in multiple myeloma cells. Blood. 2002;100:2187–94.
63. Cuendet M, Christov K, Lantvit DD, Deng Y, Hedayat S, Helson L, *et al.* Multiple myeloma regression mediated by bruceantin. Clin Cancer Res. 2004;10:1170–9.
64. Hideshima T, Anderson KC. Molecular mechanisms of novel therapeutic approaches for multiple myeloma. Nat Rev Cancer. 2002;2:927–37.
65. Garvin S, Dabrosin C. Tamoxifen inhibits secretion of vascular endothelial growth factor in breast cancer *in vivo*. Cancer Res. 2003;63:8742–8.
66. Bouclier C, Marsaud V, Bawa O, Nicolas V, Moine L, Opolon P, *et al.* Coadministration of nanosystems of short silencing RNAs targeting oestrogen receptor alpha and anti-oestrogen synergistically induces tumour growth inhibition in human breast cancer xenografts. Breast Cancer Res Treat 2009.
67. Podar K, Anderson KC. The pathophysiologic role of VEGF in hematologic malignancies: therapeutic implications. Blood. 2005;105:1383–95.
68. Barlogie B, Shaughnessy J, Tricot G, Jacobson J, Zangari M, Anaissie E, *et al.* Treatment of multiple myeloma. Blood. 2004;103:20–32.
69. Obeng EA, Carlson LM, Gutman DM, Harrington WJ Jr, Lee KP, Boise LH. Proteasome inhibitors induce a terminal unfolded protein response in multiple myeloma cells. Blood. 2006;107:4907–16.
70. Fribley A, Wang CY. Proteasome inhibitor induces apoptosis through induction of endoplasmic reticulum stress. Cancer Biol Ther. 2006;5:745–8.
71. Doisneau-Sixou SF, Sergio CM, Carroll JS, Hui R, Musgrove EA, Sutherland RL. Estrogen and antiestrogen regulation of cell cycle progression in breast cancer cells. Endocr Relat Cancer. 2003;10:179–86.
72. Caldon CE, Daly RJ, Sutherland RL, Musgrove EA. Cell cycle control in breast cancer cells. J Cell Biochem. 2006;97:261–74.
73. Bursch W, Ellinger A, Kienzl H, Torok L, Pandey S, Sikorska M, *et al.* Active cell death induced by the anti-estrogens tamoxifen and ICI 164 384 in human mammary carcinoma cells (MCF-7) in culture: the role of autophagy. Carcinogenesis. 1996;17:1595–607.